ARCHIVES OF METALLURGY

Volume 45 2000 Issue 2

TADEUSZ TELEJKO *

INVESTIGATION OF SENSITIVITY OF THE INVERSE METHOD APPLIED TO DETERMINATION OF THE THERMAL CONDUCTIVITY OF STEELS

BADANIE CZUŁOŚCI METODY WYZNACZANIA PRZEWODNOŚCI CIEPLNEJ STALI, OPARTEJ NA ROZWIĄZANIU ODWROTNYM RÓWNANIA PRZEWODZENIA CIEPŁA

In this paper the analysis of the inverse method of thermal conductivity estimation of solid body is presented. A finite element method (FEM) has been applied to study the problem. When inverse problems are involved in determination of coefficient of thermal conduction, it is necessary to measure temperature in some points of the solution domain. The proposed method has been verified by comparison of the numerical results to those obtained from the analytical solution of heat transfer equation for one-dimensional, transient heat conduction in semi-finite cylinder insulated on the circumferential surface when both boundary and initial conditions and thermal properties of the cylinder were known. Therefore, experimental data have been replaced by the temperature distribution coming from analytical formulation of the problem. Additionally it was assumed that the function of thermal conductivity dependence on the temperature belongs to class of quadractic or linear polynomials. It was found out that the method gives good and stable results in a wide range of input parameters. The set of a few temperature measurement points has been used in numerical solution. Estimation results are close to the analytical solution for varying measurement simulation times. In a domain of parameters variability neither the number nor the location of measuring points influence significantly the accuracy of thermal conductivity estimation. It has been found out that the presented method is not sensitive to the initial value of thermal conductivity used as a starting point in the model.

W artykule przedstawiono analizę metody wyznaczenia współczynnika przewodzenia ciepła ciał stałych opartą na rozwiązaniu odwrotnym równania przewodzenia ciepła. Do rozwiązania problemu zastosowano metodę elementów skończonych (FEM). Rozwiązanie problemu odwrotnego zastosowanego do wyznaczenia parametrów termofizycznych ciała wymaga pomiaru zmian temperatury w wybranych punktach. Zaproponowaną metodę zweryfikowano na podstawie znanego analitycznego rozwiązania równania przewodzenia

* WYDZIAŁ METALURGII I INŻYNIERII MATERIAŁOWEJ, AKADEMIA GÓRNICZO-HUTNICZA, 30-059 KRAKÓW, AL. MICKIEWICZA 30

ciepła dla izolowanego na pobocznicy półnieskończonego pręta. Wyznaczono pole temperatury w wybranych punktach pręta dla znanych warunków początkowych, brzegowych oraz parametrów termofizycznych ciała (w tym współczynnika przewodzenia ciepła). Dane te wprowadzono do modelu w miejsce danych eksperymentalnych. Założono, że poszukiwana przewodność cieplna jest związana z temperaturową zależnością w postaci wielomianu co najwyżej drugiego stopnia. Na podstawie obliczeń numerycznych określono optymalne wartości współczynnika przewodzenia ciepła, które następnie porównywano z dokładnym rozwiązaniem analitycznym. W wyniku przeprowadzonych testów numerycznych otrzymano wyniki wskazujące na dobrą stabilność i zbieżność zaproponowanej metody w szerokim zakresie zmienności parametrów wejściowych. Metoda pozwala na identyfikację przewodności cieplnej na podstawie pomiaru temperatury w kilku punktach położonych wewnątrz ciała. Daje dobre wyniki przy różnych czasach obliczeń, a co za tym idzie różnej ilości danych pomiarowych stanowiących podstawę identyfikacji. W badanych obszarach zmienności liczba i położenie punktów pomiarowych nie wpływa znacząco na rezultaty obliczeń numerycznych. Założenie początkowej wartości przewodności cieplnej znacznie różniące się od wartości rzeczywistej nie powoduje także błędów w rozwiązaniu.

1. Introduction

The solution of the heat conduction problems requires the knowledge of thermal properties of the body, i. e. specific heat, thermal conductivity and density. As the density determination does not, in fact, involve significant difficulties, the problem of specific heat and conduction coefficient determination is rather difficult to perform. These parameters are usually spatially and/or temperature dependent. The accuracy of thermal properties estimation highly influences the results when analyzing heat conduction process. One may find the values reported in the literature, but they usually differ from each other. A diversified chemical composition, manufacturing technology, porosity or microstructure of samples taken to investigations may be a reason of discrepancies. As an example the above data in the room temperature for nickel varies from 65 W/mK to 94 W/mK dependently on the source of information [1, 2].

The problem of the thermal conductivity determination is widely discussed in literature. Various methods have been worked out for this purpose, starting from the simple stationary ones, up to the unsteady state methods, which require very complicated and sensitive measurement equipment. The commercially used apparatuses have also been constructed to enable the thermal properties identification for industry purposes. They are commonly based on the flash method proposed by Parker [3]. The thermal diffusivity a of the flat, uniform, thermally-insulated sample is measured by putting the pulse of radiant energy at its front surface and recording the transient temperature history of the back surface. There is no necessity to know the value of the thermal energy supplied to the surface, which is the great advantage of the Parker's method. The relationship between the specific heat c_p, density ϱ and thermal conductivity λ allows the determination the last parameter assuming that the quantities ϱ and c_p are known.

$$a = \frac{\lambda}{\varrho \cdot c_p}.$$

Since thermal conductivity of metals and alloys usually depends strongly on temperature, a number of experimental tests must be carried out to estimate the heat conduction coefficient as a function of temperature. The method presented in the paper enables the evaluation based on one experiment only, which may be repeated to enlarge the accuracy of the determination.

2. The inverse problem

The direct solution of the differential heat conduction equation gives the temperature distribution in the solution domain. The solution is unique, when the boundary and initial conditions and thermal properties of the body are also known. The analytical results may be obtained only for a few geometry shapes and many other simplifications have to be made that often do not satisfy the real heating process. The numerical procedures are then involved to overcome those limitations.

Inverse problems contain the class of problems where analysis of heat-conducting material requires a determination of the unknown boundary condition or the initial temperature. These topics may serve as examples of the inverse heat conduction problems (IHCP) or backward heat conduction problems (BHCP). The special area of IHCP problems are those which deal with the thermomecanical properties identification. They are known in the literature as identification heat conduction problems (IDHCP) [5]. The interior temperature distribution has to be known additionally to solve the problem. The required data are involved to the problem formulation from the experiment. The inverse problems are more difficult that direct ones, because the are ill posed. Therefore this way of the heat conduction analysis strongly needs the application of numerical methods.

There are three basic numerical methods used in analysis of inverse identification heat conduction problems. The first one is the finite difference method (FDM), which was the most popular up to recent years [4]. The finite element method (FEM) [6] and the boundary element method (BEM) [5] are the newer ones commonly applied.

The FEM, which has been used in the presented work, is the most complicated method but also the most accurate one. It makes possible to describe thermal properties of the sample with high accuracy. The FEM, however, does not give a possibility to establish a functional dependence of the heat conduction coefficient as a function of temperature. Class of the function describing the thermal conductivity with respect to temperature has to be assumed. Coefficients of the above function are then computed by minimizing the error norm between measured and computed temperature values over a set of internal points.

3. Formulation of the problem

The preliminary investigations led by the author confirmed the possibility of inverse technique application for thermal conductivity determination of the well-conducting materials [6, 7]. The aim of the present paper is to verify the accuracy of the method and to analyze its stability over the assumed domain of some entry parameters. The experimental data has been replaced by the analytical solution of one-dimensional, transient heat conduction problem in semi-finite cylinder insulated on the circumferential surface. The equations governing this problem are as follows

$$\frac{\partial t(z,\tau)}{\partial \tau} = a\frac{\partial^2 t(z,\tau)}{\partial z^2} \qquad \tau > 0, \qquad 0 < z < \infty \tag{1}$$

with the initial and boundary conditions

$$\begin{gathered} t(z,0) = 0 \\ \frac{\partial t\, 0,\tau)}{\partial z} + \frac{\alpha}{\lambda}\left[f(\tau) - t(0,\tau)\right] = 0 \\ t(\infty,\tau) = 0, \end{gathered} \tag{2}$$

where:

t — temperature,

$a = \dfrac{\lambda}{\varrho c_p}$ — thermal diffusivity,

α — heat transfer coefficient,

λ — thermal conductivity,

ϱ — density,

c_p — specific heat.

The analytical solution of the equation (1) and (2) is given in [8]

$$t(z,\tau) =$$

$$= \int_0^\tau f(\tau-\vartheta)\left[\frac{\alpha}{\lambda}\sqrt{\frac{a}{\pi\vartheta}}\exp\left(-\frac{z^2}{4a\vartheta}\right) - a\left(\frac{\alpha}{\lambda}\right)^2 \times\right.$$

$$\left.\times\exp\left(\frac{\alpha}{\lambda}z + a\left(\frac{\alpha}{\lambda}\right)^2\vartheta\right)\operatorname{erfc}\left(\frac{z}{2\sqrt{a\tau}} + \frac{\alpha}{\lambda}\sqrt{a\tau}\right)\right]d\vartheta. \tag{3}$$

Assuming ambient temperature $f(\tau)$ as a function of time defined

$$f(\tau) = t_a\sqrt{\tau} \tag{4}$$

the equation (3) comes to the form

$$\frac{t(z,\tau)}{t_a} = \sqrt{\tau}\exp\left(-\frac{z^2}{4a\tau}\right) - \frac{z\sqrt{\pi}}{2\sqrt{a}}\operatorname{erfc}\frac{z}{2\sqrt{a\tau}} - \frac{\lambda}{2\alpha}\sqrt{\frac{\pi}{a}}\times$$

$$\times\left[\operatorname{erfc}\frac{z}{2\sqrt{a\tau}} - \exp\left(a\frac{\alpha^2}{\lambda^2}\tau + \frac{\alpha}{\lambda}z\right)\cdot\operatorname{erfc}\left(\frac{z}{2\sqrt{a\tau}}\right) + \frac{\alpha}{\lambda}\sqrt{a\tau}\right]. \tag{5}$$

When $\frac{\alpha}{\lambda} \to \infty$, the front surface temperature equals the ambient temperature

$$t(0,\tau) = t_a\sqrt{\tau}$$

and the relationship (5) can be expressed as

$$t(z,\tau) = t_a\sqrt{\tau}\exp\left(-\frac{z^2}{4a\tau}\right) - zt_0\frac{\sqrt{\pi}}{2\sqrt{a}}\operatorname{erfc}\left(\frac{z}{2\sqrt{a\tau}}\right). \tag{6}$$

The above equation served to the temperature determination over a set of points inside the body assuming $t_a = 40°\text{C}$. The calculations have been made for the values of thermal properties of the cylinder, which are relevant to the carbon steel: $c_p = 500$ J/kgK, $\varrho = 7850$ kg/m^3, $\lambda = 40$ W/mK. The results have been used in the model instead of the temperature measurements.

4. Direct solution

Heat conduction equation for a solid cylinder under non-stationary conditions in a cylindrical co-ordinated has the form:

$$\frac{\partial}{\partial r}\left(\lambda r\frac{\partial t}{\partial r}\right) + \frac{\partial}{\partial z}\left(\lambda r\frac{\partial t}{\partial z}\right) + Q - r\varrho c_p\frac{\partial t}{\partial \tau} = 0 \in V. \tag{7}$$

The temperature field can be determined from solution of Eq. (7). The boundary and primary conditions are as follows:

— on the non heated bottom end of the cylinder B_d:

$$\lambda r\left(\frac{\partial t}{\partial r}l_r + \frac{\partial t}{\partial z}l_z\right) = r\alpha_d(t_d - t) \tag{8}$$

— on the circumferential surface of the cylinder B_w:

$$\lambda r\left(\frac{\partial t}{\partial r}l_r + \frac{\partial t}{\partial z}l_z\right) = r\alpha_w(t_w - t) \tag{9}$$

— on the heated top end of the cylinder B_a:

$$t(r, z=0, \tau) = t_a(\tau). \tag{10}$$

The initial condition is assumed in the form:

$$t(r, z, \tau = 0) = t_0(r, z). \tag{11}$$

Galerkin's integration scheme and standard finite element discretisation of Eq. (7) lead to the system of linear equations:

$$\left(2 K_{ij} + \frac{3}{\Delta\tau} C_{ij}\right) t^i(\tau + \Delta\tau) = \left(-K_{ij} + \frac{3}{\Delta\tau} C_{ij}\right) t^i(\tau) - 3 F_i. \tag{12}$$

Where matrices K_{ij}, C_{ij}, and vector F_i are given by:

$$K_{ij} = \int_S \lambda r \left(\frac{\partial N_i}{\partial r}\frac{\partial N_j}{\partial r} + \frac{\partial N_i}{\partial z}\frac{\partial N_j}{\partial z}\right) dS + \int_{B_w} \alpha_w N_i N_j dB_w + \int_{B_d} \alpha_d N_i N_j dB_d$$

$$C_{ij} = \int_S \varrho c_p r N_i N_j dS$$

$$F_i = -\int_{B_w} N_i \alpha_w t_w dB_w - \int_{B_d} N_i \alpha_d t_d dB_d.$$

Solution of the system of equations (12) gives the temperature field in the sample after the time interval $\Delta\tau$ for the initial temperature of the sample t_0 and for known heat transfer coefficients on the non-heated end α_d and non-heated side surface α_w of the cylinder. Both these coefficients and factor Q in Eq. (7) are equal zero to agree with analytical formulation of the problem. The length of the cylinder has been taken long enough to satisfy the semi-finite body assumption.

5. Numerical results and discussion

The iterative procedures enable obtaining of the unknown relation between thermal conductivity and temperature when the class of function is preliminarily defined. In the present study it has been assumed, that $\lambda(t)$ is a set of polynomials

$$\lambda(t) = \sum_{i=1}^{n} w_i t^{i-1}; n \geqslant 1 \tag{13}$$

and the error norm is defined as

$$Q(\lambda) = \sum_{i=1}^{l} \sum_{j=1}^{m} [t_{i,j}^{an} - t_{i,j}^{num}]^2, \tag{14}$$

where:

$t_{i,j}^{an}$ — temperature obtained from analytical solution,
$t_{i,j}^{num}$ — numerical result,
l — number of time steps $\Delta\tau$,
m — number of internal grid points.

The Broyden-Fletcher-Goldfarb-Shanno (BFGS) variable metric method [9] has been used to solve the inverse problem. It belongs to the gradient methods i. e. it requires that the gradients of the error function be evaluated. For the first attempt it was assumed that the quadratic function is good enough to fit the $\lambda(t)$ relationship.

$$\lambda(t) = w_1 + w_2 t + w_3 t^2 . \tag{15}$$

This assumption has been made for thermal properties of metals and metallic alloys as they are usually well expressed by that kind of function. As an example one can take the results obtained by Hust and Lankford from National Bureau of Standards [10]. The following relation approximates the thermal conductivity of electrolytic iron in the temperature interval from 293 K to 1000 K

$$\lambda_{\mathrm{Fe}}(T) = 106.55 - 0.1111 \cdot T + 4 \cdot 10^{-5} \cdot T^2 \tag{16}$$

with the R coefficient equal $R = 0.9998$.
Afterwards the linear $\lambda(t)$ function was assumed

$$\lambda(t) = w_1 + w_2 t \tag{17}$$

and, finally, the value of the thermal conductivity unchanged over the temperature interval

$$\lambda(t) = w_1 \tag{18}$$

was investigated.

Calculations have been performed for a number of tests. For the first tests the following set of five internal points have been admitted (starting from the front surface of the cylinder): 8 mm, 16 mm, 24 mm, 32 mm, 40 mm. Numerical results have been obtained for several measurement simulation times τ_k. Temperature *versus* time curves for the selected period of time $\tau_k = 500$ s are presented in figure 1. Good agreement of the obtained temperatures with the analytical solution has been achieved. In figure 2 the differences between the analytical and numerical results are shown. The accuracy of the numerical computations was defined as the difference between the analytical and numerical solutions by the expression

$$\Delta t = \frac{1}{m} \sum_{i=1}^{m} \left| t_i^{an} - t_i^{num} \right| \quad \text{for } \tau = \tau_k . \tag{19}$$

The obtained values of Δt vary between 0.202 K (for $\tau_k = 5$ s) and 0.556 K (for $\tau_k = 500$ s). It can be seen that the total measurement simulation time only slightly affects the accuracy of temperature field approximation.

The thermal conductivity as functions of temperature obtained for the second-degree polynomials is presented in figure 3 and figure 4. The values of the coefficients in the equation (15) are presented in table 1. Figure 5 shows the results of numerical calculations for different time increments $\Delta\tau$. The results obtained for the linear relation expressed by equation (17) are shown in table 2 and in figure 6.

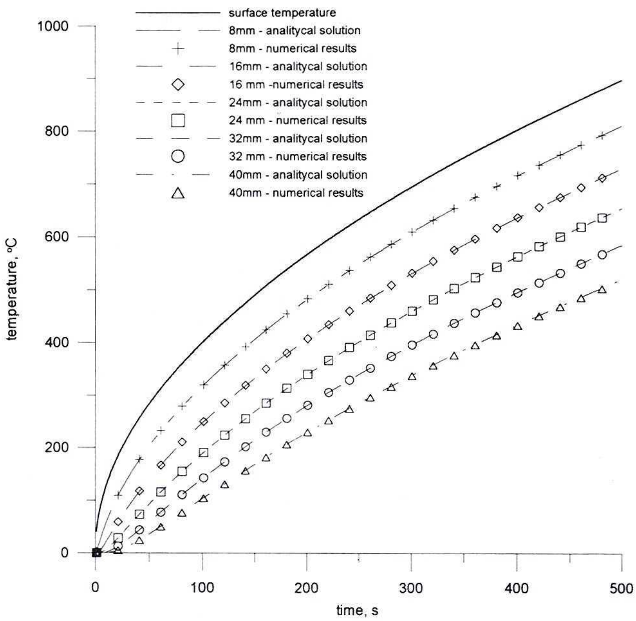

Fig. 1. Distribution of temperature at selected locations in a sample. Lines represent analytical solution, points — numerical results. The measurement simulation time is equal 500 s

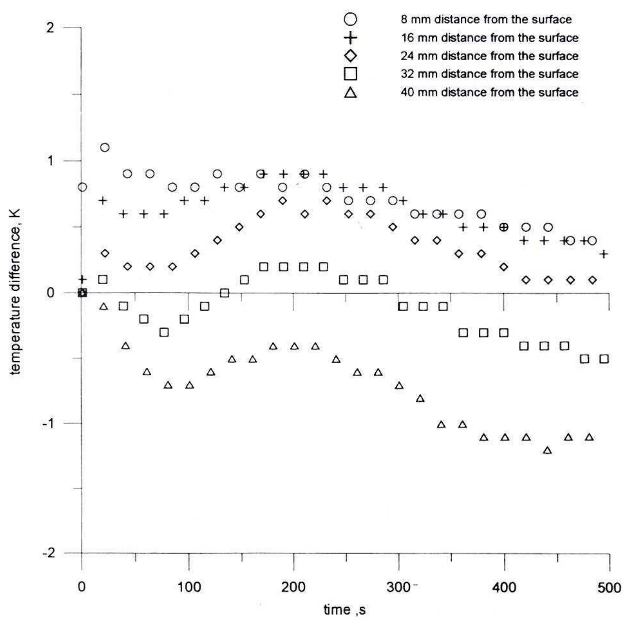

Fig. 2. Temperature differences between the computed values and those obtained from analytical solution at selected locations in the cylinder for the temperature field presented in Fig. 1

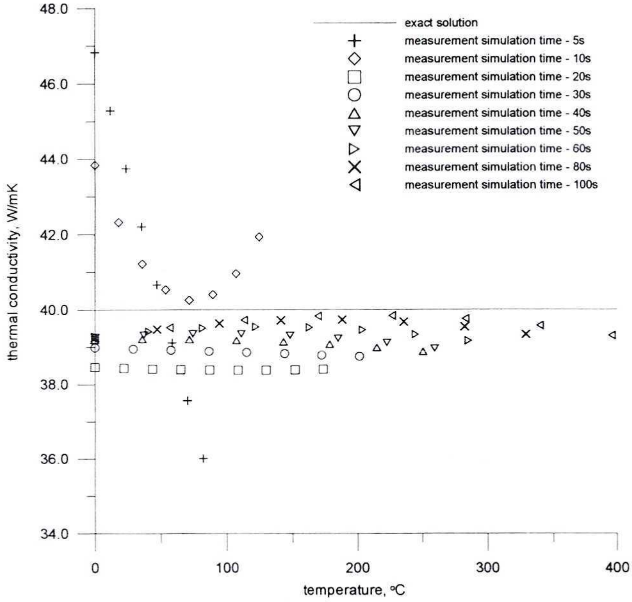

Fig. 3. Thermal conductivity dependence on the temperature for selected measurement simulation times τ_k

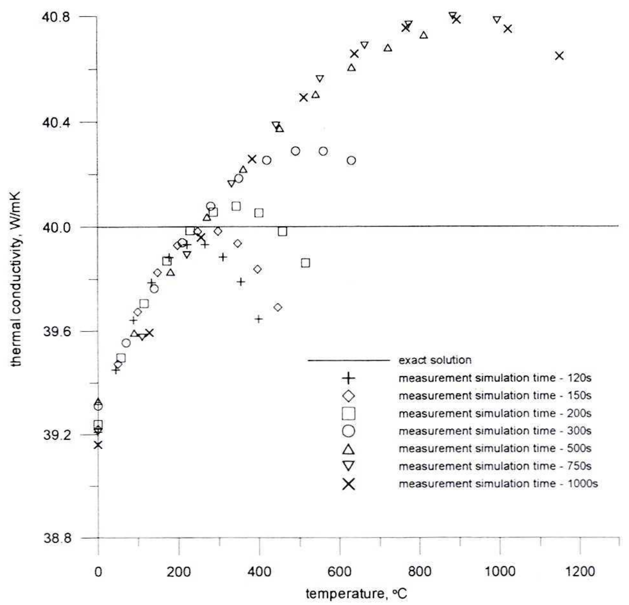

Fig. 4. Thermal conductivity dependence on the temperature for selected measurement simulation times τ_k

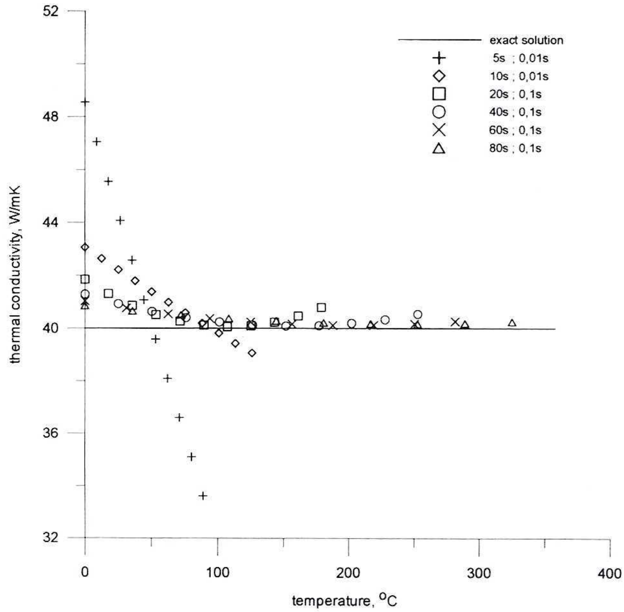

Fig. 5. The influence of time increment $\Delta\tau$ on thermal conductivity estimation. The legend presents measurement simulation time τ_k and time interval $\Delta\tau$

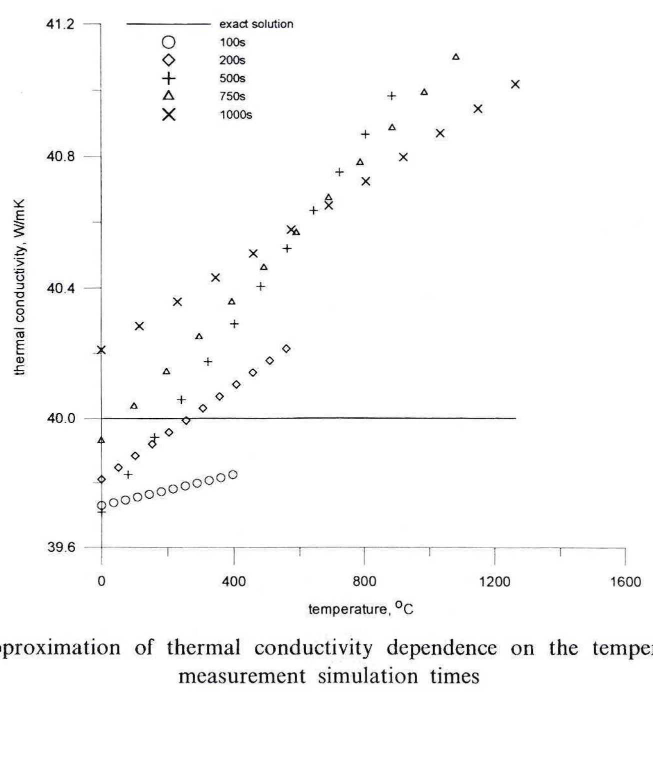

Fig. 6. Linear approximation of thermal conductivity dependence on the temperature for selected measurement simulation times

TABLE 1

Measurement simulation time	Polynomial coefficients in Eq. (9)			Temperature range from 0 to t	Error of numerical computations Δt Eq. (19)	Standard deviation S_x Eq. (20)
	w_1	$w_2 \cdot 1000$	$w_3 \cdot 1000^2$			
s	—	—	—	°C	°C	W/mK
5	46.83	−131.75	−6.22	89	0.202	0.3723
10	43.84	−97.02	654.65	126	0.225	0.1339
20	38.46	−1.5	6.63	179	0.374	0.1199
30	38.98	−1.13	−0.21	219	0.408	0.0777
40	39.19	0.76	−8.07	253	0.434	0.0561
50	39.26	2.66	−13.28	282	0.453	0.0433
60	39.28	4.05	−15.70	310	0.466	0.0347
80	39.25	5.53	−16.02	358	0.479	0.0249
100	39.23	5.97	−14.61	400	0.479	0.0198
120	39.21	5.98	−12.27	438	0.474	0.0156
150	39.22	5.6	−10.20	490	0.462	0.0136
200	39.24	4.91	−7.19	566	0.456	0.0109
300	39.31	3.75	−3.58	693	0.499	0.0109
500	39.33	3.06	−1.65	894	0.556	0.0165
750	39.21	3.52	−1.95	1095	0.504	0.0179
1000	39.16	3.65	−2.05	1265	0.441	0.0166

TABLE 2

Measurement simulation time	Polynomial coefficients in Eq. (11)		Temperature range from 0 to t	Error of numerical computations Δt Eq. (19)	Standard deviation S_x Eq. (20)
	w_1	$w_2 \cdot 1000$			
s	—	—	°C	°C	W/mK
100	39.73	0.24	400	0.490	0.0112
200	39.81	0.72	566	0.477	0.0050
500	39.71	1.44	894	0.569	0.0172
750	39.93	1.08	1095	0.563	0.0188
1000	40.21	0.64	1265	0.581	0.0185

It is worth to remind here, that the accurate solution of the inverse problem is $\lambda = 40$ W/mK. If we apply the thermal conductivity approximation error according to the following equation

$$S_x = \frac{\sqrt{\sum_{i=1}^{m} \left[\lambda(t_i^r) - \lambda(t_i^n)\right]^2}}{m}, \tag{20}$$

where:

$\lambda(t_i^r) = 40$ W/mK — accurate solution for the temperature t_i,
$\lambda(t_i^n)$ — numerical solution for the temperature t_i obtained from the relation (15), (17) or (18),
$m = \mathrm{int}(t_{\max})$ — the summation index, which is equal the integer part of the maximum temperature achieved by the first point, where temperature has been recorded in the numerical test.

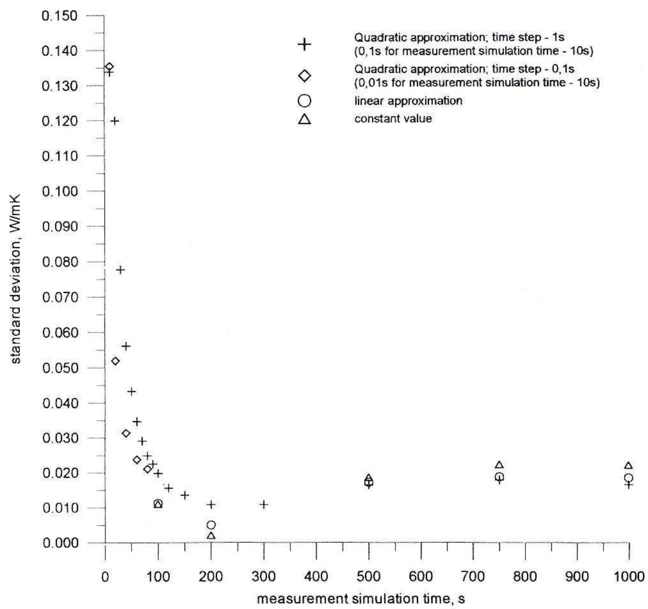

Fig. 7. Standard deviation of thermal conductivity approximation. The error for measurement simulation time equal 5 s has been omitted at the graph

Then calculated errors are shown in figure 7, table 1 and table 2. The highest value arises for the shortest measurement simulation time $\tau_k = 5$ s ($S_x = 0.3723$ W/mK) and for $\tau_k = 10$ s one gets $S_x = 0.1339$. The above-mentioned tests have been carried out with the time step $\Delta\tau = 0.1$ s. For all remaining tests ($\tau_k = 10$ s, ..., 1000 s) $\Delta\tau = 1$ s has been applied. The S_x error values fall down as τ_k goes up and do not exceed

0.2 W/mK for $\tau_k \geqslant 100$ s, which is 0.5% of the accurate solution, and are comparable to each other within the τ_k interval 100 s — 1000 s.

Figure 7 also illustrates the influence of the time interval on S_x errors. It can be seen that as $\Delta\tau$ increment decreases ten times error values also decrease but it refers just to short total times τ_k. When τ_k increases the shorter time interval does not significantly improves the accuracy of thermal conductivity approximation. Values of S_x error are still high ($S_x = 0.0314$ for $\tau_k = 40$ s) when referred to those of total times $\tau_k \geqslant 100$ s (for instance $S_x = 0.0165$ for $\tau_k = 500$ s). Comparing estimations errors for $\tau_k = 80$ s when the time steps $\Delta\tau = 1$ s and $\Delta\tau = 0.1$ s were adopted to the calculations it can be seen that there is only a little difference between them ($S_x = 0.0210$ and $S_x = 0.0249$ respectively). It can be therefore expected that the time step shortening will not essentially enlarge the convergence of numerical results to the exact ones when total calculation period τ_k increases. Further, shorter time increments always elongate computation time.

For the temperature independent coefficient of heat conduction (Eq. 12) the numerical solution is shown in table 3.

TABLE 3

Measurement simulation time τ_k, s	100	200	500	750	1000
Thermal conductivity λ, W/mK	39.78	40.05	40.56	40.74	40.79
Temperature range from 0 to t, °C	400	566	894	1095	1265
Error of numerical computations Δt, K — Eq. (19)	0.490	0.492	0.791	0.799	0.717
Standard deviation S_x, W/mK Eq. — (20)	0.0112	0.0021	0.0187	0.0224	0.0222

The highest value of the standard deviation $S_x = 0.0224$ is observed for $\tau_k = 750$ s (see table 3). It can be seen that the degree of the polynomial adopted to numerical calculations does not essentially affect accuracy of the thermal conductivity approximation for the total measurement simulation time bigger than 100 s.

The aim of the next tests was to assess, how the number of temperature measurement points and their locations inside the body affect numerical estimation results. The set of five points to record temperature has been firstly admitted. They have been marked with the numbers; 1 — is the point within 8 mm from the heated cylinder surface, 2—16 mm from the surface, 3—24 mm from the surface, etc. Afterwards one or two points have been randomly eliminated from the set. Therefore calculations have been worked out for the sets containing three or four different locations of temperature recording points. The results are presented in figure 8. The S_x errors have been also attached in the legend. The stable and good estimates of thermal conductivity have been achieved. The standard deviation is about the same for all of performed numerical test. The method gives therefore still good results even when the number of temperature sensors is reduced to four or three.

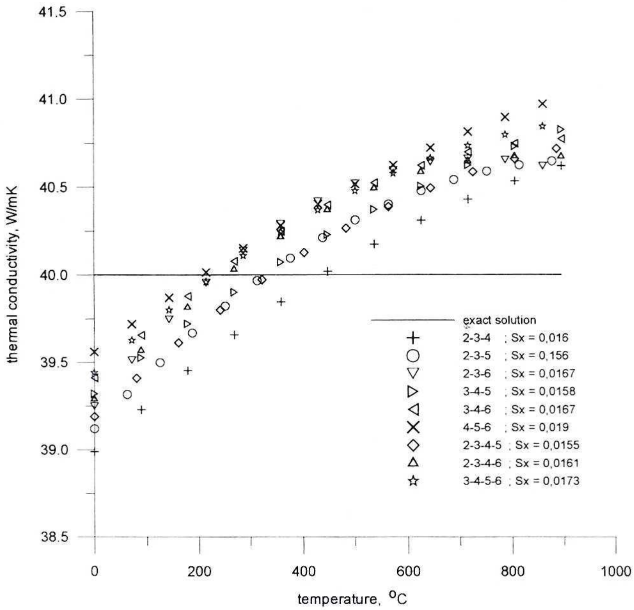

Fig. 8. Thermal conductivity *versus* temperature curves for selected number and locations of temperature measurement points. Standard deviations of numerical estimations are presented in the legend

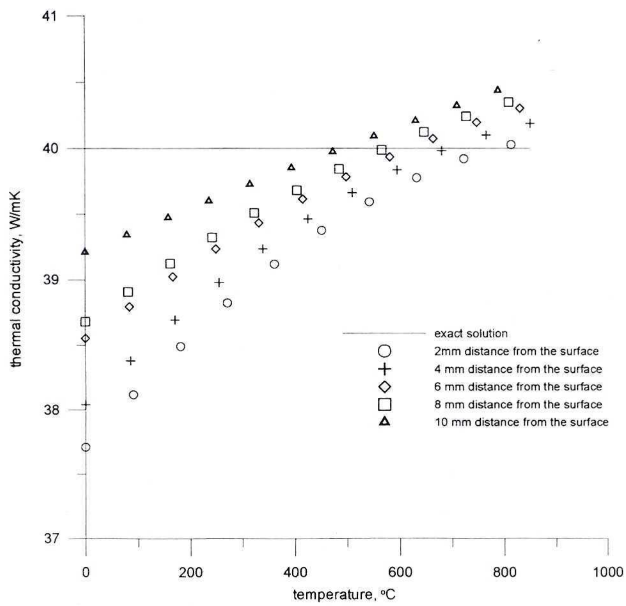

Fig. 9. Thermal conductivity dependence on the temperature for selected locations of the first temperature measurement point from the surface. The distance is the same for all points and equal 2 mm

In the following numerical tests, for the set of five points, the location of the first temperature measurement point from the surface has been moved from 2 mm to 10 mm. The distance between the points has also been changed from 2 mm up to 10 mm. The selected approximations are presented in Figs 9—13, the standard deviations of the obtained results are shown in figure 14. The analysis of the results leads to the conclusion that the estimation accuracy depends on the distance between the sensor location points and is the worst for the 2 mm distance (see Fig. 14). For the remaining tests the results do not differ much from each other. The above conclusion is confirmed by the graphs presented in Figs 15 and 16. If the location of the first point is established at a distance 2 mm from the heated surface and the distance between the rest of the points increases from 2 mm up to 10 mm, then approximation error decays. When the 6 mm distance is achieved the stabilizing of S_x error is observed. The standard deviation does not exceed 0.0160 W/mK. The better estimation results are also observed for the larger distance of the first measuring point from the heated cylinder end. In the test where it is placed at 4 mm position standard deviation reaches $S_x = 0.0311$ W/mK, whereas for the remaining tests does not exceed $S_x = 0.02$ W/mK.

In the next tests initial values of thermal conductivity included to the model have been changed within the interval between 10 and 100 W/mK. The tests have been carried out for the set of five measuring points. The final results of numerical

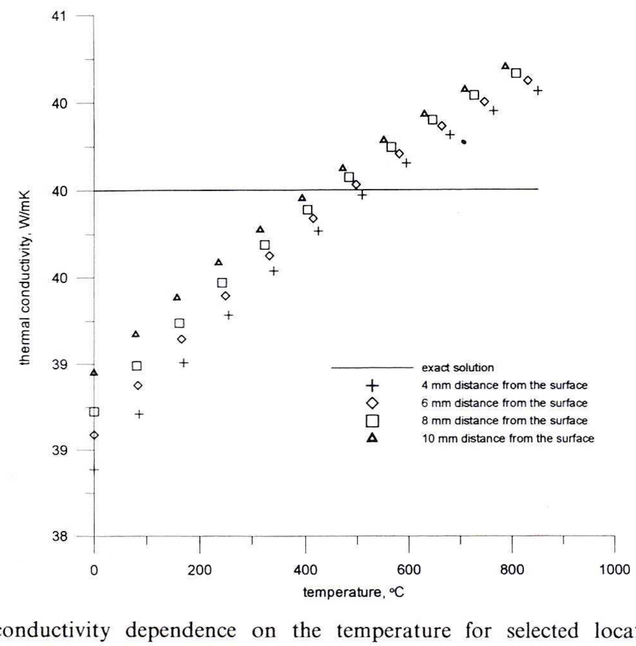

Fig. 10. Thermal conductivity dependence on the temperature for selected locations of the first temperature measurement point from the surface. The distance is the same for all points and equal 4 mm

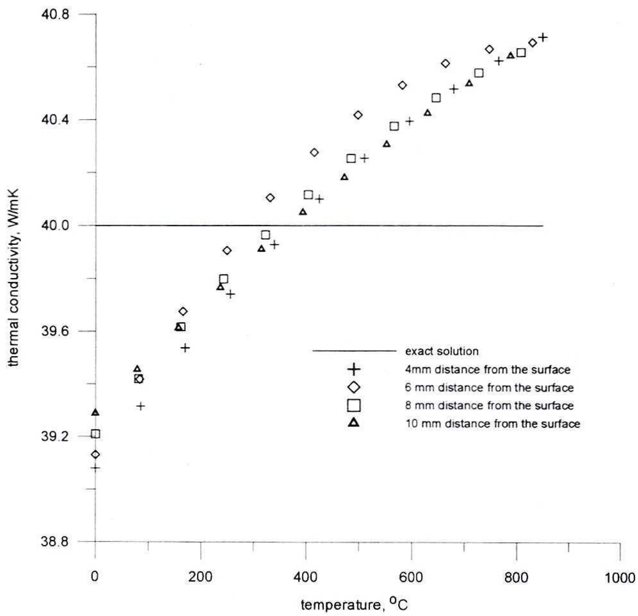

Fig. 11. Thermal conductivity dependence on the temperature for selected locations of the first temperature measurement point from the surface. The distance is the same for all points and equal 6 mm

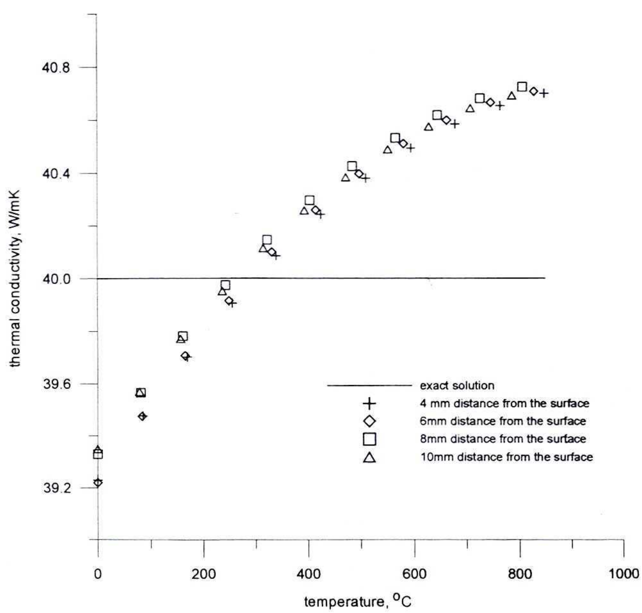

Fig. 12. Thermal conductivity dependence on the temperature for selected locations of the first point from the surface. The distance is the same for all points and equal 8 mm

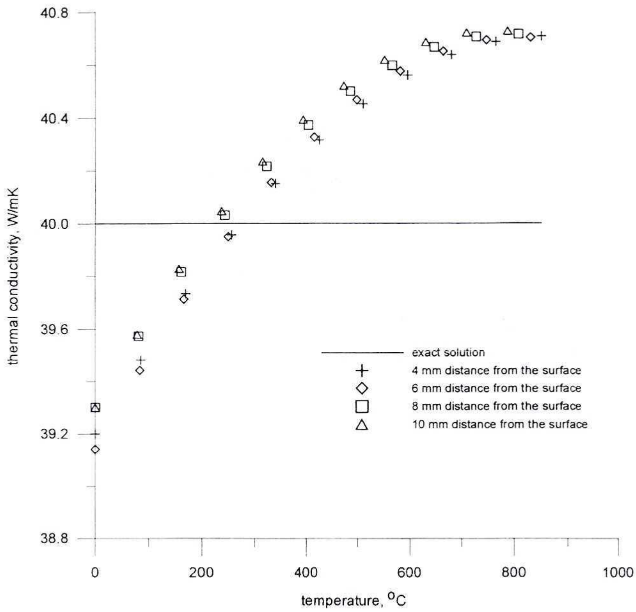

Fig. 13. Thermal conductivity dependence on the temperature for selected locations of the first temperature measurement point from the surface. The distance is the same for all points and equal 10 mm

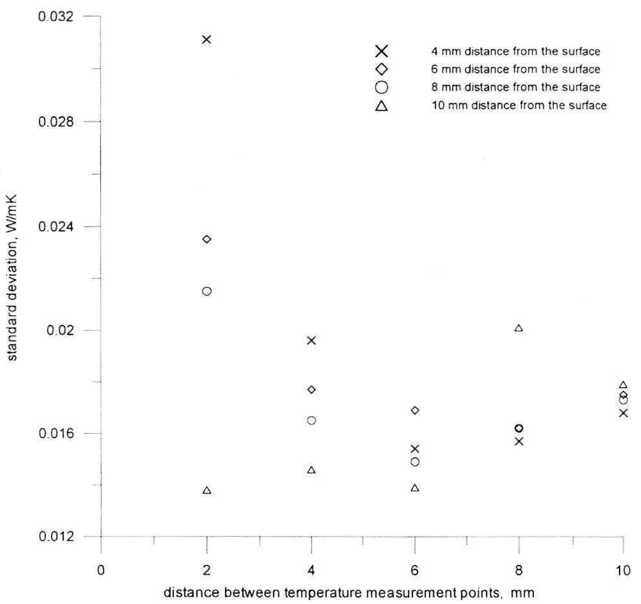

Fig. 14. Accuracy of thermal conductivity approximation for different locations of the first temperature measurement point

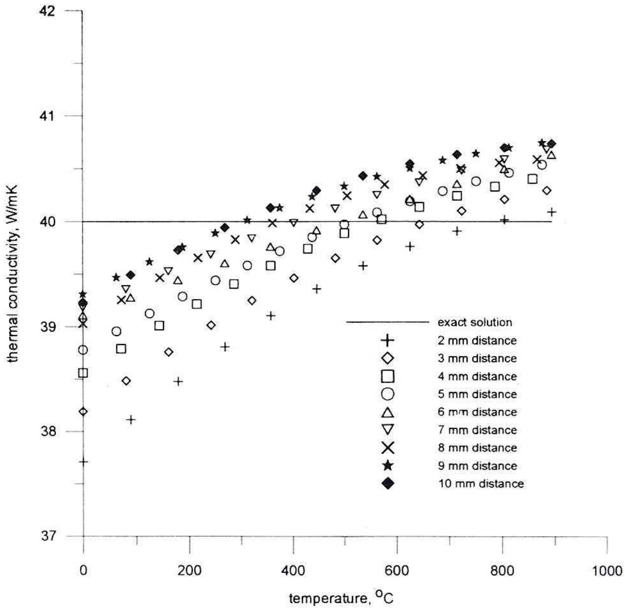

Fig. 15. Thermal conductivity dependence on the temperature for different distances between temperature measurement points. Distance from the first measuring point to the surface is equal 2 mm

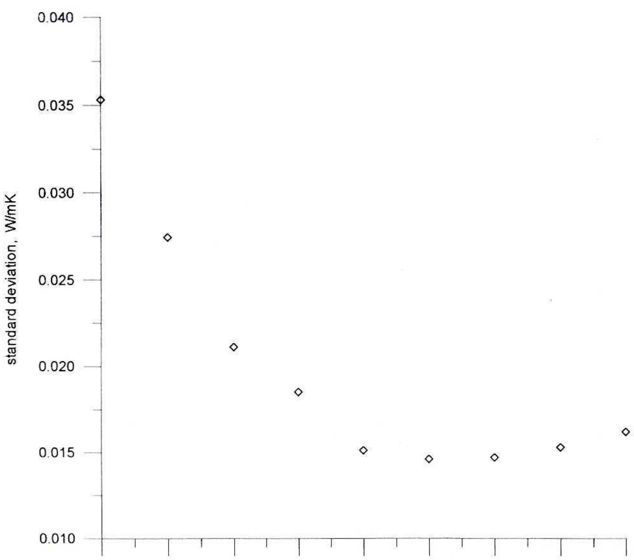

Fig. 16. Accuracy of thermal conductivity approximation for different distances between temperature measurement points. The first point is located 2 mm from the surface

calculations are pictured in figure 17. The legend to the figure contains the standard deviations of approximation. There is no perceptible difference both for the thermal conductivity determination and standard deviations for all the performed tests. Therefore, the method produces very good and stable results apart from the initial coefficient of heat conduction involved to the numerical procedure.

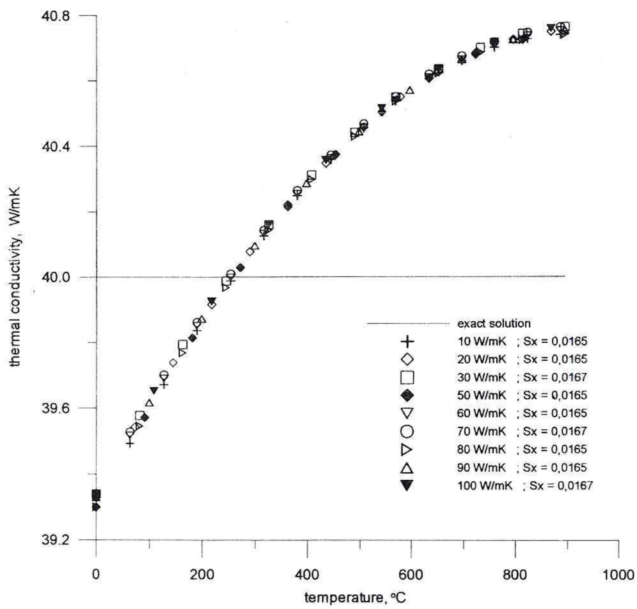

Fig. 17. Thermal conductivity dependence on the temperature and standard deviation of approximation for different initial values used as a starting point in numerical computations

Since there are no analytical solutions of the heat conduction equation for the temperature dependent thermal conductivity and heat capacity, the numerical results have been used to verify the method. The temperature distribution in the semi-finite cylinder has been calculated form the direct model assuming that both thermal conduction and specific heat are quadratic functions of temperature. First the numerical direct solution has been checked by comparing the results of a number of temperature calculations to those obtained in analytical way for constant conductivity and heat capacity. The presented examples of numerical computations have been performed for the following parameters: $c_p = 500$ J/kgK, $\varrho = 7850$ kg/m^3, $\lambda = 60$ W/mK for a couple of measurement simulation times τ_k. The input temperature field to the model has been obtained from Eq. (6) assuming $t_a = 40$°C. The errors of numerical results are collected in table 4; the differences between analytical and numerical temperature distribution are shown in figure 18.

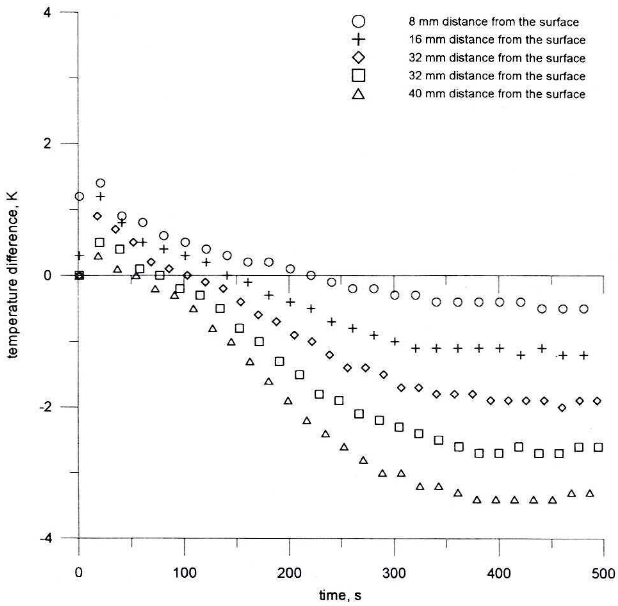

Fig. 18. Temperature differences between the results of direct problem and those obtained from analytical solution at selected locations in the sample

TABLE 4

Measurement simulation time τ_k, s	100	200	500	750	1000
Temperature range from 0 to t, °C	331	496	823	1024	1193
Error of numerical computations Δt, K Eq. (19)	0.607	0.629	1.445	1.581	1.555

The numerical results for the temperature inside the solution domain show good estimates of the corresponding analytical solution. The biggest difference in results does not exceed 3.5 K and the mean error Δt computed from Eq. (19) is not higher than 1.6 K.

The temperature field has been obtained from the direct solution for the following $\lambda(t)$ and $c_p(t)$ functions

$$\lambda(t) = 42.43 - 41.76 \cdot 10^{-3} t + 16.52 \cdot 10^{-6} t^2 \qquad \text{W/mK}$$
$$c_p(t) = \lambda(t) = 472.4 + 93.57 \cdot 10^{-3} t + 576.62 \cdot 10^{-6} t^2 \qquad \text{J/kgK}.$$

The results served as a temperature measurement simulation for the inverse calculations. Two sets of coefficients as an initial guess in Eq. (9) have been used in the model to investigate the convergence of the method. Table 5 contains the computed polynomial parameters for $\tau_k = 500$ s and five temperature measurement points placed every 8 mm from each other. It can be seen that initial guess does not influence the results of calculations in the presented examples. The method gives the results, which are of the excellent agreement with the exact solution. The errors are by far smaller than the accuracy of temperature measurements.

TABLE 5

Parameters of equation 9	Exact solution	Starting point: $w_1 = 40$ $w_2 = 40 \cdot 10^{-3}$ $w_3 = 40 \cdot 10^{-6}$	Starting point: $w_1 = 20$ $w_2 = 4 \cdot 10^{-3}$ $w_3 = 4 \cdot 10^{-6}$	Starting point: $w_1 = 60$ $w_2 = 0$ $w_3 = 0$
w_1	42.43	42.43	42.43	42.43
w_2	$-41.76 \cdot 10^{-3}$	$-41.77 \cdot 10^{-3}$	$-41.77 \cdot 10^{-3}$	$-41.77 \cdot 10^{-3}$
w_3	$16.52 \cdot 10^{-6}$	$16.53 \cdot 10^{-6}$	$16.53 \cdot 10^{-6}$	$16.53 \cdot 10^{-6}$
Temperature range from 0 to t, °C	748	748	748	748
Error of numerical computations Δt, K — Eq. (19)	—	0.026	0.026	0.026

6. Conclusions

The present study has investigated the inverse problem of thermal conductivity determination using the FEM from the additional time temperature measurements, which have been taken at arbitrary defined locations in the heated body. The set of five measurement points is included to the model, which guarantee the high accuracy of the results. The properties of the body involved to the model are typical for the carbon steels. The constant, linear or second-degree polynomial may be applied to estimate thermal conductivity *versus* temperature. The method gives good, stable and convergent results for the wide range of investigated parameters. The total measurement simulation time τ_k and the location of measurement points affect the accuracy of the results. The best agreement between analytical and numerical tests has been achieved for $\tau_k \geqslant 100$ s and for the distance between the measurement points at least 6 mm. The thermal conductivity approximation is also better for the first measurement point located at least 6 mm from the heated surface. The time step used in numerical calculation impacts the estimation accuracy in the limited way. This has been observed exlusively for the total measurement simulation time shorter than 80 s. For the longer time the shortening of $\Delta\tau$ increment does not significantly improve the thermal conductivity determination. It has been found out that the presented method is not sensitive to the initial value of thermal conductivity used as a starting point in the model. The algorithm has been also tested for the temperature dependent thermal conductivity and heat capacity of the sample. The excellent agreement between the results obtained from a direct solution and the inverse method has been found out.

The observations made in this study may be helpful in determination of the terms of experiment, which ensure the best results of thermal conductivity estimation.

The financial support by Scientific Research Committee (KBN) of Poland is gratefully acknowledged. University of Mining and Metallurgy, Faculty of Metallurgy and Material Science, grant No 10.10.110.250.

REFERENCES

[1] K. Rażniewicz, Tablice cieplne z wykresami, WNT, Warszawa 1966.
[2] A. S. Ochotin, Tepłoprowodnost' twierdych tieł — sprawocznik, Energoatomizdat, Moskwa 1984.
[3] W. J. Parker, R. J. Jenkins, C. P. Butler, G. L. Abbot, Flash Method of Determining Thermal Diffusivity, Heat Capacity, and Thermal Conductivity, Journal of Applied Physics **32,** 9, 1679—1684 (1961).
[4] R. Cerny, J. Toman, A Difference Method for Determining the Thermal Conductivity of Porous Materials in a Wide Temperature Range, High Temperatures-High Pressures **29,** 51—57 (1997).
[5] D. Lesnic, L. Elliot, D. B. Ingham, Identification of the Thermal Conductivity and Heat Capacity in Unsteady Noinlinear Heat Conduction Problems Using the Boundary Element Method, Journal of Computational Physics **126,** 410—420, (1996).
[6] Z. Malinowski, A. Buczek, T. Telejko, S. Słupek, Określenie współczynnika przewodzenia ciepła metodą rozwiązania odwrotnego, Materiały IV Konferencji. Zastosowanie komputerów w zakładach przetwórstwa metali, 1997, Ustroń-Jaszowiec, pp. 199—206 (in Polish).
[7] T. Telejko, Z. Malinowski, A. Buczek, Analysis of the Inverse Solution in Application to Determining Thermal Conductivity of Metals, Metallurgy and Foundry Engineering **23,** 3, 177—185 (1998).
[8] Lykow, Teorija teploprovodnosti, GTTI, Moskwa 1952.
[9] T. Kręglewski, T. Rogowski, A. Ruszczyński, J. Szymanowski, Metody optymalizacji w języku FORTRAN, PWN, Warszawa 1984.
[10] J. G. Hust, A. B. Lankford, Report of Investigation Research Materials 8420 and 8421, National Bureau of Standards, Gaithersburg, May 1984.

REVIEWED BY: PROF. DR HAB. INŻ. MACIEJ PIETRZYK

Received: 12 April 2000.